

Unstable yet static initial state: A universal method for studying Rayleigh-Taylor instability and lock exchange

Kazuya U. Kobayashi* and Rei Kurita†

*Department of Physics, Tokyo Metropolitan University, 1-1 Minamioosawa,
Hachioji-shi, Tokyo 192-0397, Japan*



(Received 22 July 2018; published 24 January 2019)

Macroscopic flow induced by instability is a feature found in both natural phenomena and industrial processes; however, *in situ* observation of instabilities at an early stage in their formation is rare. In this article, we propose an experimental method for observing the early stages of a Rayleigh-Taylor instability and lock exchange. We successfully used physical gels to form a “static” initial state which is simultaneously “gravitationally” unstable. Fluid instabilities can be observed from the beginning by switching from a static state to a dynamic state by irradiating the system with light. We can also observe flow dynamics under arbitrary boundary conditions using this method. Here we present notable results in the early stages of a Rayleigh-Taylor instability and lock exchange. Our method promises to greatly advance experimental research into many types of instability phenomena, contributing to the elucidation of nonequilibrium phenomena in fluids.

DOI: [10.1103/PhysRevFluids.4.013901](https://doi.org/10.1103/PhysRevFluids.4.013901)

I. INTRODUCTION

Fluid flow is intimately linked to changes in physical properties like concentration and temperature and thus plays an important role in macroscopic physical phenomena. Phenomena driven by fluid dynamics are frequently observed in daily life and in industrial processes [1,2]. We especially note that nonequilibrium phenomena accompanied by hydrodynamic instability are related not only to fluid mechanics, but also to fields such as supernovae, plasma science (nuclear fusion), geophysics, and astrophysics. Hydrodynamic instabilities have thus been extensively investigated [3–12].

A particular example of this occurs when a heavy fluid lies over a lighter fluid in a constant gravitational field, causing fluctuations at the interface to grow exponentially and generating macroscopic flow; this is called a Rayleigh-Taylor instability. The early stages of Rayleigh-Taylor instabilities have predominantly been studied using theoretical and numerical simulations. At an early stage, it is known that fluctuations with the most unstable wavelength λ tend to grow dramatically. Many descriptions for λ have been proposed; however, they are considered only in a limited condition, although Rayleigh-Taylor instability occurs in a variety of situations. [1,3,4,12,13]. Regardless of how it is understood, there are notably few experimental studies of λ in the early stages of instability formation. For those that exist, it has thus far been impossible to eliminate artificial perturbations on the interface [9,14,15]. For example, withdrawing a partition between two fluids induces large artificial flow. One can initiate rotation for an entire experimental system from a stable state, but this is inappropriate for low-viscosity fluids. When two liquids are miscible, this

*kobayashi-ukai@tmu.ac.jp

†kurita@tmu.ac.jp

experiment is doubly unfeasible, as it is not possible to prepare a sharp interface to begin with since the interface becomes diffuse with time.

A lock-exchange flow is another important example of macroscopic flow induced by a density difference [16–19]. When two fluids with different densities come in contact with each other horizontally, the higher density fluid slides under the lower density fluid. It is also reported that a Kelvin-Helmholtz instability (shear-driven fluid instabilities) occurs at the interface in the initial stage of this process. The relevance of this phenomenon to meteorological and magnetohydrodynamic phenomenon has been discussed [20,21]. In experiments, two fluids are horizontally separated by a partition (lock gate) [17,19]. When the lock gate is removed, it is not possible to avoid perturbations, and a strong shear stress is applied to the fluid. Again, it is extremely difficult to experimentally observe the early stages of lock-exchange flow.

Thus, it is clear that an accurate experimental study for the early stages of (i) a Rayleigh-Taylor instability and (ii) a lock-exchange flow is sorely necessary. Here we propose an experimental method for preparing a static initial interface despite an “gravitationally” unstable state, which can be used to observe the early stages of an instability. Furthermore, we also show how this method can be applied to easily visualize flow under arbitrary boundary conditions. We note that this method is ubiquitous, allowing a detailed study of the early stages thanks to its accuracy, versatility, and easy application. We hope that experiments using this method will progress our understanding of nonequilibrium phenomena related to hydrodynamics.

II. EXPERIMENT

Methods and materials

We used gelatin purchased from Wako Pure Chemical Industries Co., Ltd., and made 5 wt% and 6 wt% concentration gelatin solutions using pure water as a solvent. The densities of the two gelatin solutions are $\rho_5 = 1.04 \text{ g/cm}^3$ (5 wt%) and $\rho_6 = 1.09 \text{ g/cm}^3$ (6 wt%). The sol-gel transition temperatures T_s are 27°C for 5 wt% and 28°C for 6 wt% determined by the falling ball method [22,23]. It is known that the viscosity changes by roughly 100 times with a difference of several $^\circ\text{C}$ near T_s . Since the density change is small for the sol-gel transition of gelatin, the flow induced by the volume change is negligible. It is known that the gelatin solution is a Newtonian fluid above the sol-gel transition temperature [24]. Thus, we can investigate the Rayleigh-Taylor instability and lock-exchange flow of Newtonian fluids. We use rhodamine 6G purchased from Wako Pure Chemical Industries to visualize the flow field. We also used silicone oil (KF-96L-1cs, $\rho_s = 0.82 \text{ g/cm}^3$, kinematic viscosity of $1 \text{ mm}^2/\text{s}$) manufactured by Shin-Etsu Chemical Co., Ltd. Then we describe the sample preparation method. First, the gelatin solution is heated to 40°C , where it is in a sol state; this is then injected into the sample cell. Next, it is cooled in the refrigerator to gel. Then a dense fluid is gently poured onto the gelatin in the gel state. Due to the elasticity of the gel state, the energetically unstable state persists for at least 2 h at room temperature.

A schematic of the experimental setup is shown in Fig. 1. Our sample chambers are quasi two-dimensional Hele-Shaw cells for facile analysis of the flow. We performed experiments with a glass sample chamber with internal dimensions (H, L, W) = (30 mm, 126 mm, 2.4 mm). The sample chamber is heated without any physical contact by irradiation with light from the back; the gel state transforms into a sol state on heating. The light is defocused with a cylindrical lens so that it uniformly irradiates the sample surface. Black paper is attached to the surface to improve the heating efficiency. To create artificial boundary conditions, we attached the black paper to the area to be fluidized only, while covering the rest with insulating materials. Instability phenomena can be observed in the region coated with black paper, all the way from the initial to final stages of the process. Temperature is measured using a radiation thermometer (FT-H10, KEYENCE Co.) and a contact thermometer (AD-5602A, A&D Company, Ltd.) for inside the gelatin. The room temperature is set to 20.3°C with a standard air conditioner for our experiment; the final sample temperature after the experiment is about 29°C . These images were recorded with a digital camera (Model HC-V520M, Panasonic Co.).

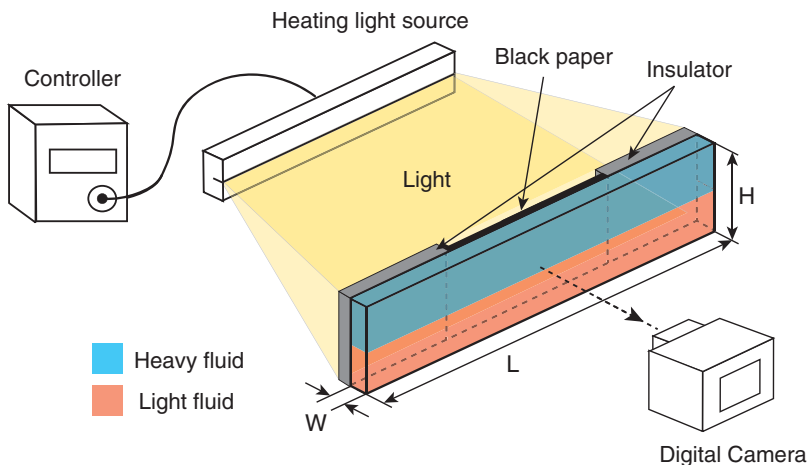


FIG. 1. A schematic of our experimental setup. We performed the experiment with glass sample chambers with internal dimensions $(H, L, W) = (30 \text{ mm}, 126 \text{ mm}, 2.4 \text{ mm})$. The sample chamber is heated using light irradiation from the back. In order to improve the efficiency of heating, black paper is attached to the area to be heated; the rest is covered with insulating materials.

III. RESULTS AND DISCUSSION

A. How to observe an early stage of instabilities

First, we propose an experimental method to prepare a static initial state, despite being in an “gravitationally” unstable state. To begin, we focus on the Rayleigh-Taylor instability. The experimental apparatus is shown as in Fig. 1. The bottom liquid (lower density liquid) is a gelatin solution in a gel state; we can use any liquid for the upper layer liquid so long as it is heavier than the gelatin solution, e.g., gelatin solution with a higher concentration. Gelatin solution is a typical

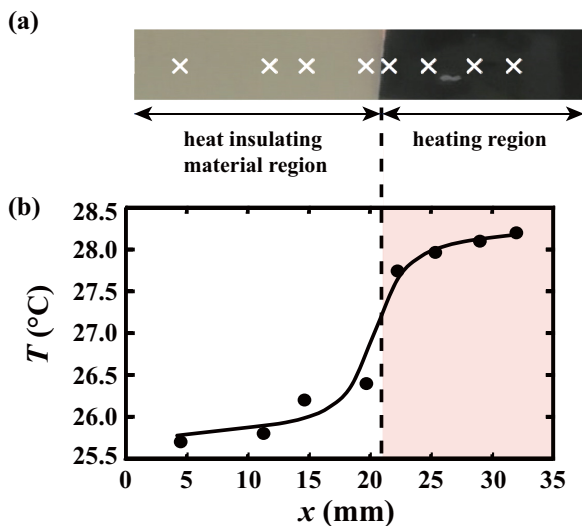


FIG. 2. (a) An enlarged image near a boundary between a heating region and a heat-insulating region. Cross symbols are measured points of the temperature by a thermometer. (b) The spatial dependence of the temperature near the boundary. The length of the boundary effect was less than 5 mm from the boundary.

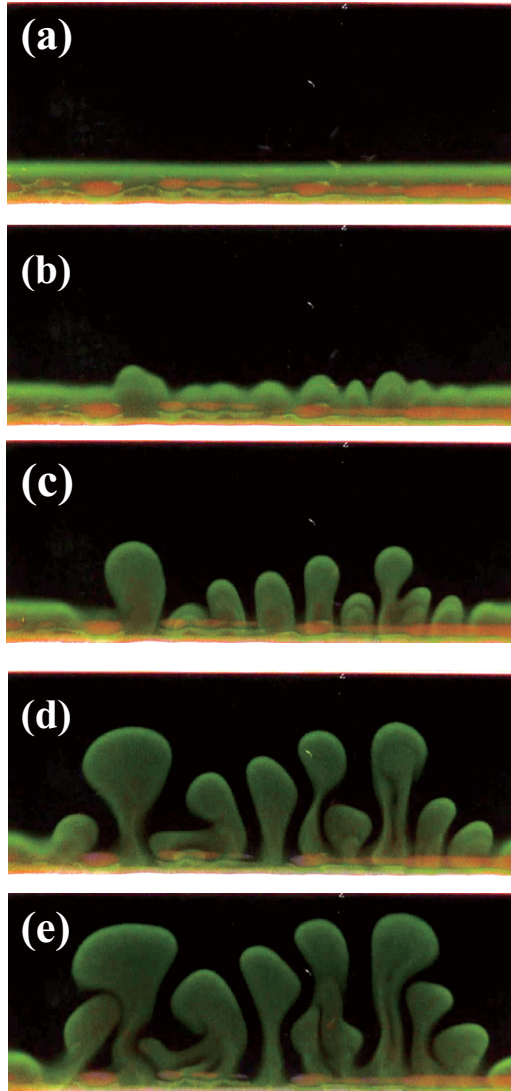


FIG. 3. The time evolution of the Rayleigh-Taylor instability in the gelatin solution at (a) $t = 0$ s, (b) $t = 71$ s, (c) $t = 138$ s, (d) $t = 214$ s, and (e) $t = 260$ s. The horizontal length of the images corresponds to 70 mm. The green region corresponds to the 5 wt% gelatin solution, and the black region corresponds to the 6 wt% gelatin solution. The orange region is background, unrelated to the flow. A stationary, flat interface is realized in a density inverted state (a). The instability starts by heating with light from the back (b). A fingering pattern grows over time (c–e).

example of a physical (thermoreversible) gel; it can be reversibly transformed from an elastic gel (solid) state to a sol (liquid) state by changing the temperature [22,23]. The gel state lacks fluidity and is able to sustain its shape due to its elasticity. Even when a gel and another miscible liquid are in contact, diffusion does not occur since the timescale of the diffusion is extremely long. Therefore, we can prepare a stationary interface even though the system is gravitationally unstable.

At the beginning of the experiment, the sample is uniformly heated to above the sol-gel transition temperature using a strong light, irradiating the back of the sample cell. We set $t = 0$ when the interface starts to fluctuate. We measure that the whole sample is heated homogeneously with

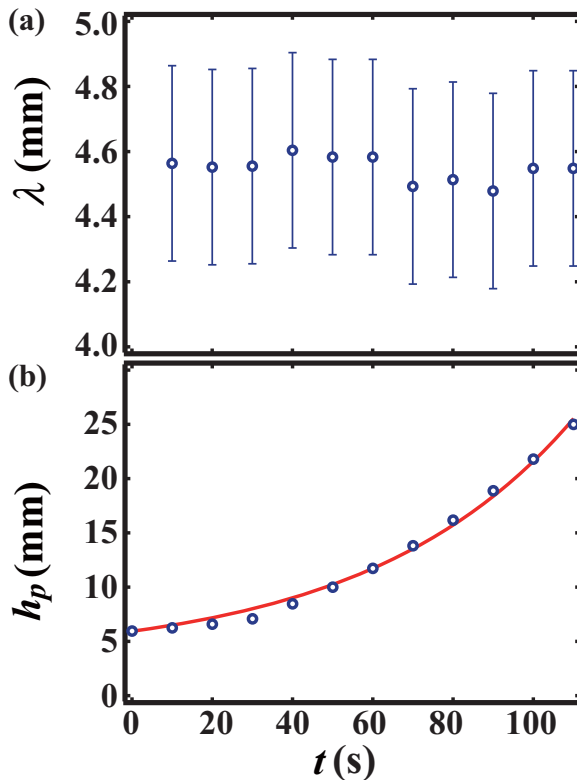


FIG. 4. The time evolutions of (a) the most unstable wavelength λ and (b) the amplitude of the fluctuations h_p at $h_b = 5.9$ mm. λ is constant, and h_p exponentially grows. Those are typical behaviors of Rayleigh-Taylor instability in the early stage. The error bar in panel (a) comes from a distribution of the fluctuation. The solid line in panel (b) is a fitting line by the exponential curve.

a heating rate of $1^\circ\text{C}/\text{min}$, with a spatial fluctuation of $\pm 0.1^\circ\text{C}$. In addition, we also measured the temperature gradient across the thickness of the sample cell. We prepared the gelatin solution 10 wt% with $W = 7.2$ mm thickness and then put a contact thermometer inside the gelatin. During the heating, we found that the temperature difference is less than 0.1°C along the thickness below $T = 30^\circ\text{C}$. Thus, the gel in the bottom layer transforms into a sol state simultaneously, and a Rayleigh-Taylor instability arises. This method is capable of capturing the initiation of the instability phenomenon without any artificial perturbation, while traditional techniques such as rotation and withdrawal of a horizontal partition cause unavoidable flow. We note again that the gelatin solution is a Newtonian liquid above the sol-gel transition temperature. Thus we can investigate the instability between the Newtonian liquids. In addition, we can systematically vary the viscosity difference, density difference, and surface tension by freely choosing the upper liquid. We note here that our method is limited in the liquid-liquid Rayleigh-Taylor instability. In the Hele-Shaw cell, we find that wetting to side glasses occurs, and then it is difficult to investigate the gas-liquid Rayleigh-Taylor instability.

In order to investigate the effect of different boundary conditions and initial conditions, we use a heat-insulating material to cover the sample chamber except for the experimental region. When exposed to light, only the experimental region is heated by the light. Then we measured the temperature near the boundary between the heating region and the heat-insulating region. Figure 2(a) shows an enlarged image near a boundary between a heating region and a heat-insulating region. Cross symbols are measured points of the temperature with a thermometer. We found that

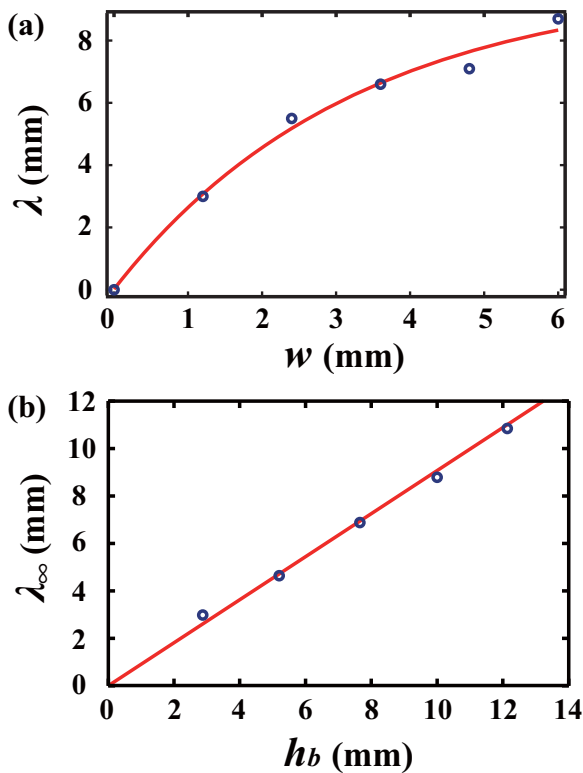


FIG. 5. (a) λ as a function of W at $h_b = 10$ mm. λ increases exponentially with W . (b) λ_∞ as a function of h_b . λ_∞ linearly increases with h_b .

the temperature difference is about 1.5°C near the boundary as shown in Fig. 2(b). Since viscosity exponentially increases with decreasing temperature near the sol-gel transition temperature, mobility of the liquid is significantly different between the heating region and the heat-insulating region. Thus the boundary is regarded as the nonslip wall. The temperature difference induces large mobility difference near the sol-gel transition temperature. Though the heat is conducted to the surroundings, since heating via the light is much faster than the conduction, we can observe the early stages of the instability inside the experimental region. In addition, the material transfer due to the thermal flow (Ludwig-Soret effect) can be also neglected since the mobility is quite low at the boundary.

B. Early stage of the Rayleigh-Taylor instability

Here we investigate the early stages of Rayleigh-Taylor instabilities between two gelatin solutions with different concentrations (see movie 1 in the Supplemental Material [25]). We use 6 wt% ($\rho_6 = 1.09 \text{ g/cm}^3$) for the upper layer and 5 wt% ($\rho_5 = 1.04 \text{ g/cm}^3$) for the bottom layer. Since both fluids are gelatin solutions with a small concentration difference, the interfacial tension should be extremely small. Such conditions are the most difficult to investigate when considering the early stages of Rayleigh-Taylor instabilities. We heat an area with a width of $L = 70$ mm using a heat-insulating material to prevent heat transport to other regions. We measured the temperature near the boundary between the heating region and the heat-insulating region. The temperature difference is about 1.5°C near the boundary between the heating region and the heat-insulating region (see Fig. 2). Since mobility exponentially decreases at the heat-insulating region, the boundary in this experiment resembles a nonslip boundary condition. For visualization, the low-density fluid layer (5 wt%) is dyed with rhodamine 6G. In Fig. 3(a) we can see that a stationary, flat interface is realized,

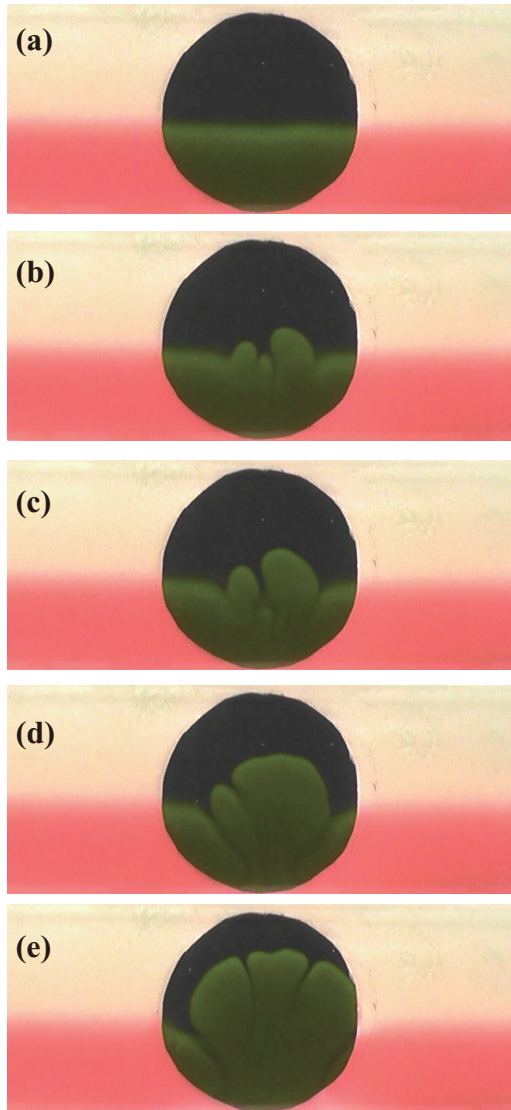


FIG. 6. The time evolution of the Rayleigh-Taylor instability with circular boundary conditions at (a) $t = 0$ s, (b) $t = 380$ s, (c) $t = 435$ s, (d) $t = 650$ s, and (e) $t = 1028$ s. The diameter of the circle is 30 mm. The rest is covered with a heat insulator. The green and orange regions correspond to a 5 wt% gelatin solution. The black and white regions correspond to the 6 wt% gelatin solution. A ginkgo leaf pattern is formed inside the circle, while nothing changes outside the circle.

despite a density-inverted state. This state is stable for more than 3 h at 20 °C. The instability due to the density difference is induced by quick heating to above the sol-gel transition temperature using the light. When both gelatin solutions transform from the gel state to the sol state, we observe a small disturbance at the interface due to Rayleigh-Taylor instability [Fig. 3(b)]. This finger pattern grows over time and is consistent with previous work [Figs. 3(c)–3(e)].

Here we measure time evolutions of the most unstable wavelength λ and a maximum height of the bottom layer h_p . We obtain the most unstable wavelength λ as a distance between peaks of the fluctuations. We averaged λ over the number of the peaks N_p . N_p is 10–20 in our experiment. The

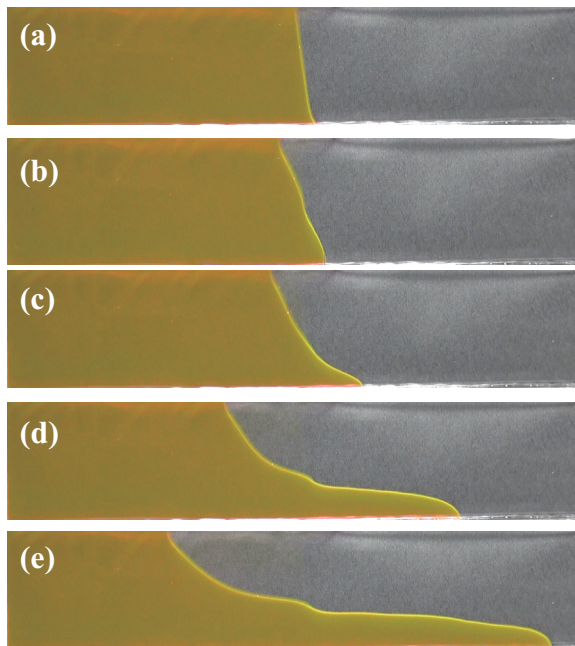


FIG. 7. The time evolution of lock-exchange flow between two fluids, using 6 wt% gelatin solution (orange) and silicone oil (black) at (a) $t = 0$ s, (b) $t = 50$ s, (c) $t = 121$ s, (d) $t = 183$ s, and (e) $t = 239$ s. We successfully form a stationary, vertical, flat interface without a traditional lock gate (a). A lock-exchange flow is subsequently driven by the density difference (b–e).

time evolution of λ and h_p when a thickness of the bottom layer h_b is 5.9 mm as shown in Fig. 4. We find that λ is constant with time. The error bar comes from the distribution of the wavelength. Meanwhile, h_p exponentially grows with $h_p = 3.27 + 2.62 \exp(t/51.4)$ for $h_b = 5.9$ mm. The constant λ and the exponential growth of the fluctuations are typical features for the early stage of the Rayleigh-Taylor instability [3,4].

Then we investigate λ with changing the thickness of the Hele-Shaw cell W . Figure 5(a) shows λ as a function of W at $h_b = 10$ mm, and we find that λ increases exponentially. We fit λ with $\lambda = \lambda_\infty [1 - \exp(-W/\xi)]$, where λ_∞ and ξ are the most unstable wavelength at $W = \infty$ and a typical thickness of the Hele-Shaw cell, respectively. We obtain that λ_∞ and ξ are 9.9 mm and 3.7 mm, respectively. Previous articles reported that $\lambda = CW$ and C is 2–5 [26–28]. We obtain that $\lambda \approx CW$ in the small W regime and C is 2.68. Thus our result is consistent with the previous results in the small W regime [26–28]. We also investigate λ_∞ as a function of h_b shown as in Fig. 5(b). It is found that λ_∞ linearly increases as $\lambda_\infty = h_b$.

Here λ is sometimes estimated using $\lambda \approx 4\pi(v^2/A_T g)^{1/3}$, where A_T , v , and g are the Atwood number $A_T = (\rho_H - \rho_L)/(\rho_H + \rho_L)$, $v = (\eta_H + \eta_L)/(\rho_H + \rho_L)$ of two fluids, and acceleration due to gravity, respectively [1,3,4]. ρ_H and η_H are density and viscosity of the high density fluid, respectively, and ρ_L and η_L are density and viscosity of the low-density fluid, respectively. From this equation, λ is estimated to be 29 mm. Although this equation neglects the interfacial tension and seems to fit our experimental conditions, the estimate is inconsistent with our result. Meanwhile, according to Whitehead and Luther [13], $\lambda = 6.98h_b$ when a ratio of both fluids' viscosities is close to 1. Although the exponent of h_b is consistent with our experiment results, the estimated λ is 7 times larger than λ_∞ in our experiment. In addition, the growth rate n is estimated to be 8.2 s^{-1} from the analytical equation, which $n = 0.149g(\rho_H - \rho_L)h_b/\eta_L$ [13]. It is also inconsistent with our result (0.019 s^{-1}). The analytical equation assumes that the viscosity is quite high, while viscosity

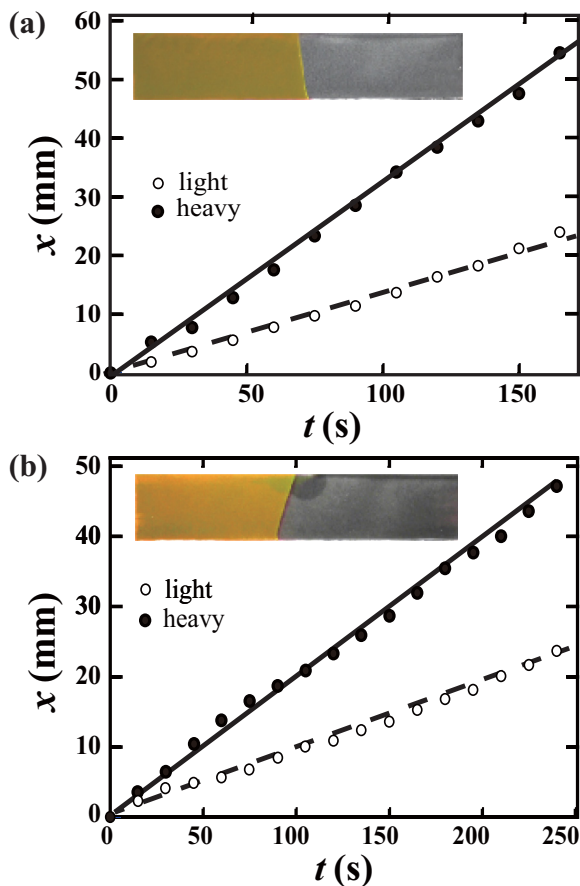


FIG. 8. Distances between the front position of the fluid and the initial position at (a) $\delta\theta > 0$ and (b) at $\delta\theta < 0$. We find that the front of the fluid moves with constant velocity.

of the sol state of the gelatin solution is low ($0.05 \text{ Pa} \cdot \text{s}$) in our experiment. Increasing viscosity would damp out instabilities at shorter wavelengths since the damping strength by dissipation term is proportional to $\nu\lambda^{-2}$. Therefore, the wavelength of instability estimated by the theory with high viscosity would be larger than that observed in a system with low viscosity. Thus we consider that observations of microscopic flow in the early stage are needed to clarify the relation between λ and h_b . It may be also interesting to investigate the unstable wavelength systematically in the early stages by varying the viscosity ratio and the density ratio. We note that our method can be extended to such experiments.

C. Rayleigh-Taylor instability in a specific boundary condition

We can also investigate the time evolution of the Rayleigh-Taylor instability under a circular boundary condition as shown in Fig. 6 (see movie 2 in the Supplemental Material [25]). As shown in Figs. 6(a) and 6(b), an interface destabilization occurs and a fingering pattern grows. Here note the difference with Fig. 3: the fingering pattern spreads rather than growing vertically [Figs. 6(c) and 6(d)]. The flow in the circular boundary condition is slower than that in bulk, thus the diffusion also plays an important role for the pattern growth. In the later stage, the pattern spreads larger than the most unstable wavelength, and then new fingers with downward flow appear on the top of the pattern. As a result of coupling between hydrodynamics and diffusion, a ginkgo leaf pattern

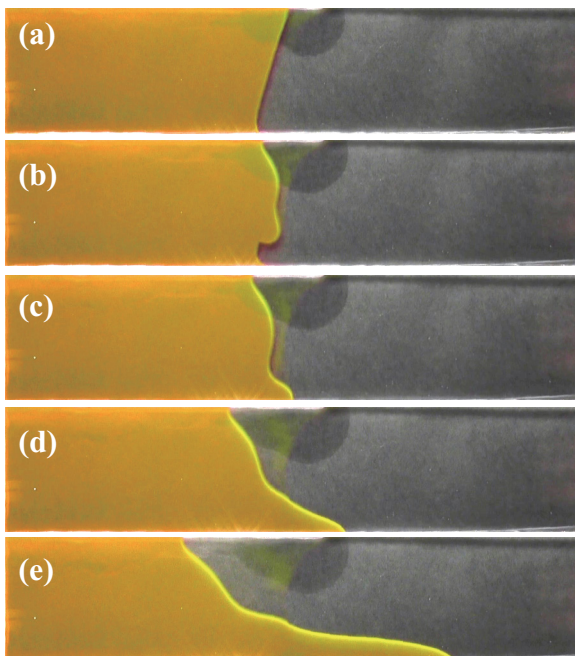


FIG. 9. Time evolution of the lock-exchange flow in 6 wt% gelatin solution (orange) and silicone oil (black) with an inclined interface. (a) $t = 0$ s, (b) $t = 83$ s, (c) $t = 112$ s, (d) $t = 164$ s, and (e) $t = 240$ s. We also realized the formation of an inclined stationary flat interface without a traditional lock gate (a). The gelatin solution surges over the silicone oil; this is significantly different behavior compared to flow with a vertical interface (b–c). The gelatin solution then slides into the silicon oil in a similar manner to the vertical interface system (d–e). The front velocity of the gelatin solution is much higher than with a vertical interface.

is formed. In this manner, we can easily investigate the flow dynamics under arbitrary boundary conditions by changing the shape of the heat insulator. In general, it is known that flow patterns strongly depend on boundary conditions; therefore, the versatility of our method is expected to contribute significantly to the development of fluid dynamics.

D. Transition in a lock-exchange experiment

Next, we looked at another prototypical example, performing a lock-exchange experiment. We used a 6 wt% gelatin solution ($\rho_6 = 1.09 \text{ g/cm}^3$) and silicone oil ($\rho_s = 0.82 \text{ g/cm}^3$). For visualization, we dyed the gelatin solution with rhodamine 6G. We succeed in creating a vertical, stationary, and flat interface without a partition, as shown in Fig. 7(a). Since the gelatin solution is in a gel state, the flat interface can be maintained for at least 3 h. By heating the entire system above the sol-gel transition temperature, the gel is fluidized [Fig. 7(b)]. The gelatin solution then begins to flow downward, and the silicone oil starts flowing upward [Figs. 7(c)–7(e)].

Then we measure time evolutions of fronts of both layers. We find that the front moves with constant velocity as shown in Fig. 8(a). The front velocity V of the silicone oil is 0.11 mm/s, while that of the gelatin solution is 0.19 mm/s. Here we find that dynamics of the front of the two fluids are asymmetric. This is consistent with a numerical simulation study, which reports that the front velocity of the higher density fluid is higher than that of the lower density fluid [17,29].

It is also possible to accurately characterize lock exchange with an inclined interface. Figure 9(a) shows a stationary interface in which the high-density fluid is inclined toward the low-density fluid. After heating with the light, we find that the gelatin solution surges over the silicon oil [Figs. 9(b) and 9(c)]. This early flow is quite different from the flow shown in Fig. 7(a). The gelatin solution

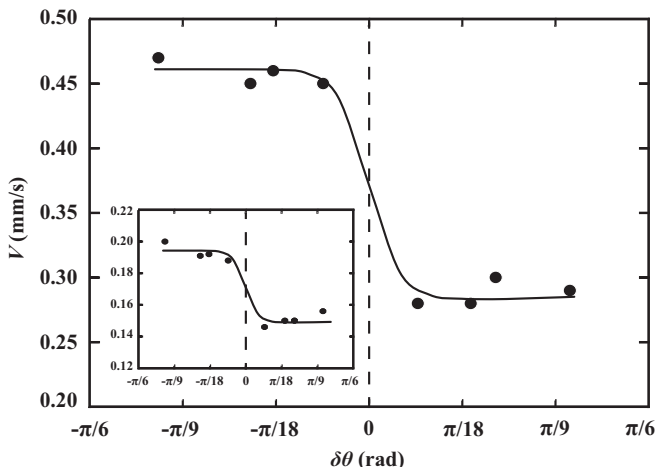


FIG. 10. V of the heavier fluid as a function of $\delta\theta$. A transition of V can be observed at $\delta\theta = 0$. It is also found for V of the lighter fluid shown as an inset.

subsequently slides and moves under the silicone oil [Figs. 9(d) and 9(e)]. Figure 8(b) shows the distances between the front position of the fluid and the initial position with an inclined interface. Here we measured the front velocities and found that the silicone oil moved at 0.15 mm/s, while the gelatin solution moved at 0.33 mm/s. We find that the front velocity is faster than that in the lock exchange with the flat interface.

Then we investigate the angle dependence of the velocity. We define the angle θ as an angle of the interface from the horizontal axis. We set the direction of θ in order that the interface between two fluids is stable if $\theta = 0$, while the Rayleigh-Taylor instability occurs when $\theta = \pi$. Figure 10 shows V of the heavier fluid as a function of $\delta\theta$, where $\delta\theta = \theta - \pi/2$. When θ is positive, V of the heavier fluid is about 0.28 mm/s, on the other hand, V drastically increases across $\delta\theta = 0$, where the high-density fluid is inclined toward the low-density fluid (see Fig. 9). It is also found for V of the lighter fluid shown as the inset in Fig. 10. Here we extract the front shapes of the heavier liquid by the image analysis. Tips of the heavier liquid are overlapped in Fig. 11. The blue solid line and the blue dashed line correspond to the front shape at $t = 183$ s and 239 s at $\delta\theta > 0$, while the red solid line and the red dashed line correspond to the front shape at $t = 164$ s and 240 s at $\delta\theta < 0$.

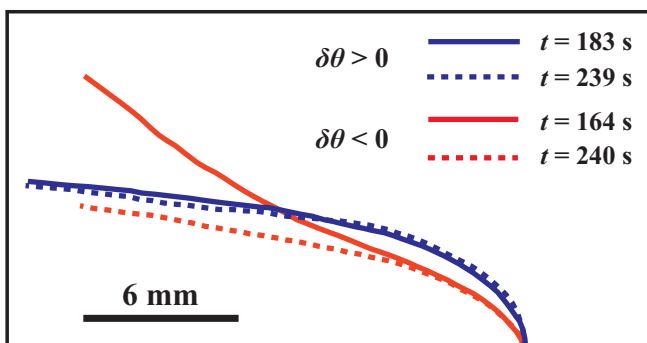


FIG. 11. The front shapes of the heavier liquid extracted by the image analysis. The blue solid line and the blue dashed line correspond, respectively, to the front shape at $t = 183$ s and 239 s at $\delta\theta > 0$, while the red solid line and the red dashed line correspond, respectively, to the front shape at $t = 164$ s and 240 s at $\delta\theta < 0$. Tips of the heavier liquid are overlapped. The front shape is more streamlined for $\delta\theta < 0$.

solid line and the red dashed line correspond to the front shape at $t = 164$ s and 240 s at $\delta\theta < 0$. We find that the front shape is unchanged with time; however, the front shape is more streamlined for $\delta\theta < 0$. Thus V becomes faster for $\delta\theta < 0$ since the velocity is determined by the force balance between the viscose force and the gravitational force.

This means that the initial condition (the angle of the interface) affects the flow in the early stages of the instability; this initial flow subsequently influences the flow in later stages. This is the first experimental evidence for flow in the early stages of shape formation affecting macroscopic flow in the later stages, a phenomenon contradicted by conventional wisdom. We can expect that more aspects of lock-exchange flow will be revealed through systematic studies of the interfacial tension, the viscosity difference, and the density difference, using this simple, versatile method.

IV. CONCLUSION

We propose an experimental method for investigating Rayleigh-Taylor instability and lock exchange combining light and a physical gel. We succeeded in forming static initial conditions despite being “gravitationally” unstable. We successfully observed a Rayleigh-Taylor instability from the earliest stages in a low interfacial tension system, even using circular boundary conditions. We find that the most unstable wavelength in our experiment is inconsistent with any theoretical predictions. In a lock-exchange flow, it was experimentally found that the front velocity shapely varies depending on the angle of the initial interface. This is experimental evidence for flow in the early stages affecting macroscopic flow at latter stages. Our method enables the realization of static initial condition and arbitrarily complex boundary conditions, the most crucial factors for flow dynamics. We thus hope that our method will be able to realize further experimental research into the fluid instability phenomenon, particularly the fluid dynamics associated with instabilities.

ACKNOWLEDGMENTS

K.U.K. was supported by the JSPS Research Fellowship for Young Scientists (17J03066). R.K. was supported by JSPS KAKENHI (16K13865) and (17H02945).

-
- [1] S. Chandrasekhar, *Hydrodynamic and Hydromagnetic Stability* (Dover Publications, New York, 1981).
 - [2] N. I. Kolev, *Multiphase Flow Dynamics I* (Springer, Berlin, 2005).
 - [3] D. L. Youngs, Numerical simulation of turbulent mixing by Rayleigh-Taylor instability, *Physica D* **12**, 32 (1984).
 - [4] D. H. Sharp, An overview of Rayleigh-Taylor instability, *Physica D* **12**, 3 (1984).
 - [5] H. J. Kull, Theory of the Rayleigh-Taylor instability, *Phys. Rep.* **206**, 197 (1991).
 - [6] G. A. Houseman and P. Molnar, Gravitational (Rayleigh–Taylor) instability of a layer with non-linear viscosity and convective thinning of continental lithosphere, *Geophys. J. Int.* **128**, 125 (1997).
 - [7] W. H. Cabot and A. W. Cook, Reynolds number effects on Rayleigh–Taylor instability with possible implications for type Ia supernovae, *Nat. Phys.* **2**, 562 (2006).
 - [8] C. Völtz, W. Pesch, and I. Rehberg, Rayleigh-Taylor instability in a sedimenting suspension, *Phys. Rev. E* **65**, 011404 (2001).
 - [9] J. L. Vinningland, Ø. Johnsen, E. G. Flekkøy, R. Toussaint, and K. J. Måløy, Granular Rayleigh-Taylor Instability: Experiments and Simulations, *Phys. Rev. Lett.* **99**, 048001 (2007).
 - [10] R. S. Craxton, K. S. Anderson, T. R. Boehly, V. N. Goncharov, D. R. Harding, J. P. Knauer, R. L. McCrory, P. W. McKenty, D. D. Meyerhofer, J. F. Myatt *et al.*, Direct-drive inertial confinement fusion: A review, *Phys. Plasmas* **22**, 110501 (2015).
 - [11] K. A. Baldwin, M. M. Scase, and R. J. A. Hill, The inhibition of the Rayleigh-Taylor instability by rotation, *Sci. Rep.* **5**, 11706 (2015).

- [12] M. A. Gallis, T. P. Koehler, J. R. Torczynski, and S. J. Plimpton, Direct simulation monte carlo investigation of the Rayleigh-Taylor instability, *Phys. Rev. Fluids* **1**, 043403 (2016).
- [13] J. A. Whitehead and D. S. Luther, Dynamics of laboratory diapir and plume models, *J. Geophys. Res.* **80**, 705 (1975).
- [14] S. B. Dalziel, Rayleigh-Taylor instability: Experiments with image analysis, *Dyn. Atmos. Oceans* **20**, 127 (1993).
- [15] M. S. D. Wykes and S. B. Dalziel, Efficient mixing in stratified flows: Experimental study of a Rayleigh-Taylor unstable interface within an otherwise stable stratification, *J. Fluid Mech.* **756**, 1027 (2014).
- [16] C. Härtel, E. Meiburg, and F. Necker, Analysis and direct numerical simulation of the flow at a gravity-current head. Part 1. Flow topology and front speed for slip and no-slip boundaries, *J. Fluid Mech.* **418**, 189 (2000).
- [17] R. J. Lowe, J. W. Rottman, and P. F. Linden, The non-Boussinesq lock-exchange problem. Part 1. Theory and experiments, *J. Fluid Mech.* **537**, 101 (2005).
- [18] V. K. Birman, J. E. Martin, and E. Meiburg, The non-Boussinesq lock-exchange problem. Part 2. High-resolution simulations, *J. Fluid Mech.* **537**, 125 (2005).
- [19] G. P. Matson and A. J. Hogg, Viscous exchange flows, *Phys. Fluids* **24**, 023102 (2012).
- [20] H. Hasegawa, M. Fujimoto, T.-D. Phan, H. Reme, A. Balogh, M. W. Dunlop, C. Hashimoto, and R. TanDokoro, Transport of solar wind into earth's magnetosphere through rolled-up Kelvin-Helmholtz vortices, *Nature (London)* **430**, 755 (2004).
- [21] D. M. Schultz, K. M. Kanak, J. M. Straka, R. T. Trapp, B. A. Gordon, D. S. Zrnić, G. H. Bryan, A. J. Durant, T. J. Garrett, P. M. Klein, and D. K. Lilly, The mysteries of mammatus clouds: Observations and formation mechanisms, *J. Atmos. Sci.* **63**, 2409 (2006).
- [22] K. U. Kobayashi, N. Oikawa, and R. Kurita, Dynamical transition of heat transport in a physical gel near the sol-gel transition, *Sci. Rep.* **5**, 18667 (2015).
- [23] K. U. Kobayashi, N. Oikawa, and R. Kurita, Thermal convection in a thermosensitive viscous fluid with inhomogeneous cooling, *J. Phys. Soc. Jpn.* **86**, 043402 (2017).
- [24] R. Wulansari, J. R. Mitchell, J. M. V. Blanshard, and J. L. Paterson, Why are gelatin solutions Newtonian? *Food Hydrocolloids* **12**, 245 (1998).
- [25] See Supplemental Material at <http://link.aps.org/supplemental/10.1103/PhysRevFluids.4.013901> for movies of Rayleigh-Taylor instability.
- [26] J. Fernandez, P. Kurowski, L. Limat, and P. Petitjeans, Wavelength selection of fingering instability inside Hele-Shaw cells, *Phys. Fluids* **13**, 3120 (2001).
- [27] E. Lajeunesse, J. Martin, N. Rakotomalala, and D. Salin, 3D Instability of Miscible Displacements in a Hele-Shaw Cell, *Phys. Rev. Lett.* **79**, 5254 (1997).
- [28] S. Harada, M. Kondo, K. Watanabe, T. Shiotani, and K. Sato, Collective settling of fine particles in a narrow channel with arbitrary cross-section, *Chem. Eng. Sci.* **93**, 307 (2013).
- [29] T. Bonometti, S. Balachandar, and J. Magnaudet, Wall effects in non-Boussinesq density currents, *J. Fluid Mech.* **616**, 445 (2008).